ArF Imaging Modeling by Using Resist Simulation and Pattern Matching

Mosong Cheng and Andrew Neureuther
Department of Electrical Engineering and Computer Sciences
University of California
Berkeley, CA 94720-1772
Phone: (510) 642-8897, Fax: (510) 642-2739
Email: mosong@eecs.berkeley.edu

ABSTRACT

This paper presents a methodology for calibrating projection printing imaging/resist models and applying the calibrated models to line-end shortening simulations in the presence of image imperfections. A scheme for extracting monochromatic representations of resist patterns from SEM pictures and comparing them with simulated images is presented. Based on this scheme, a 2-dimensional metric for evaluating the simulation performance is defined and a framework for tuning simulation models is built. The experiments were conducted on a 193nm scanner, with a binary mask whose CD's were measured to eliminate the mask error effects. Comparison of the simulated resist patterns to the SEM micrographs allows evaluation of various levels of physical assumptions on simulation models over the defocus range. Several models were evaluated to quantify the impact of lens aberrations and resist characters on pattern fidelity. Then the effectiveness of these models was further validated by applying the models to simulate small patterns. Aberration effects were found to be very distinctive and a tuned resist modeling was also found to be essential for small features.

Key words: ArF, chemically amplified resist, simulation, line-end shortening, image mismatching factor, optimization

I. INTRODUCTION

ArF resist imaging is rapidly maturing and a predictive modeling capacity that includes both the chemically-amplified resist and imaging quality is needed to guide manufacturing. To accurately describe the scanner/resist system, several systematic error factors have to be addressed, such as mask error, resist response to defocus, lens imperfection, etc. A physical lithographic model is expected to resolve these complications and predict printed patterns effectively. The pattern distortion effects, such as corner rounding and line-end shortening (LES), which are exacerbated in the extension of optical lithography into deep 100-nm regime, are increasingly important in ensuring lithographic quality, and conventional single number metrics such as critical dimension (CD) of a feature may not be adequate. Thus it is desired to quantitatively describe LES with a 2-dimensional metric and, using this metric, evaluate and optimize the simulation models.

Historically, many efforts have been made in modeling projection optics and deep-UV resists and simulating LES. T. Brunner found that the degree of LES was a strong function of line width [1]. C. Mack et al developed PROLITH, a widely accepted lithography simulator, and applied PROLITH in modeling line end shortening [2]. SOLID-C, a widely used lithography simulator developed by SIGMA-C Co, has proved very useful for 2D developed-resist image problems. J. Byers presented several methodologies in calibrating chemically amplified resist models [3]. At Berkeley, M. Zuniga proposed a non-Ficken-diffusion resist model [4], based on which two post exposure bake (PEB) simulators, STORM and RIAR, were developed by E. Croffie [5] and M. Cheng [6]. A physical model of LES using SPLAT and STORM was thereafter developed by M. Cheng [7].

In this paper, an algorithm for extracting monochromatic representation of resist patterns from SEM pictures is initially presented and then a scheme for comparing the experimental resist patterns with simulated images is discussed. Image Mismatching Factor (IMF), a 2-dimensional metric for evaluating the simulation model performance, is also defined. A framework for tuning simulation models is then built based on optimizing IMF. On the basis of the above methodology, several levels of physical assumptions in simulation models were optimized and their IMF's were compared. These models were then applied to a much smaller pattern to evaluate their predictabilities. The impact of factors leading to pattern feature distortion, including lens aberrations, resist optical and PEB parameters, on IMF are then discussed.

II. EXTRACTING MONOCHROMATIC RESIST PATTERNS FROM SEM

In general, the SEM pictures are 256-gray-scaled images. In order to quantitatively calculate the difference between SEM pictures and simulated images, it is necessary to quantize the SEM pictures into 2 levels, or white and black, which correspond to remaining resist and cleared region, respectively. The algorithm for making SEM pictures monochromatic is described as below:

Step 1: Edge detection. Given a gray-scaled SEM picture, denoted as $I = (I_{mn})$, $1 \le m \le M$, $1 \le n \le N$, where M and N are the height and width of the image in number of pixels. Assume the image has 256 gray levels, i.e., $0 \le I_{mn} \le 255$, 0 corresponds to the darkest pixels and 255 corresponds to the brightest pixels. The edges of the resist patterns are usually the brightest pixels in a SEM picture. Therefore the edge detector can be defined as a threshold detector:

$$D[I, Th] = J = (J_{mn}), J_{mn} = \begin{cases} 1 & \text{if } I_{mn} > Th \\ 0 & \text{if } I_{mn} \le Th \end{cases} \tag{1}$$

Here *Th* is a predetermined threshold. After edge detection, the SEM image *I* is converted into a monochromatic image *J*, in which 1's are the edges of the resist patterns, as is depicted in Fig. 1(b).

Step 2: Noise removal. As can be seen in Fig. 1(b), there are some random pixels in *J* whose values are 1. They can be removed by an averaging filter [2] followed by a threshold detector:

$$K = J * H, H = \frac{1}{12}\begin{pmatrix} 1 & 1 & 1 \\ 1 & 4 & 1 \\ 1 & 1 & 1 \end{pmatrix} \tag{2}$$

Here "*" is convolution. *H* is the moving average window matrix [8].

$$L = D[K, NT] = (L_{ij}), L_{ij} = \begin{cases} 1 & \text{if } K_{mn} > NT \\ 0 & \text{if } K_{mn} \le NT \end{cases} \tag{3}$$

Here *NT* is also an adjustable threshold between noise and real edges. In this paper *NT* is taken as 0.5. The image after noise removal is shown in Fig. 1(c).

Step 3: Filling the region inside the edges. It is desired to differentiate the remaining resist from the cleared region by assigning the pixels of the dark region the value of 1 while assigning other pixels the value of 0. There have been many mature filling-area algorithms. In this paper the simplest scan-line polygon fill algorithm [9] was employed. The image after filling was shown in Fig. 1(d). Denote the image as P.

Step 4: Clipping proper image. Generally only a particular part of the SEM image is of interest. As is in Fig. 1(d), only the region outlined by the dotted lines is needed to compare with simulation, because it is the critical feature of this pattern. The clip of interest is characterized by the coordinates of its center, (x_0, y_0), which is termed " alignment mark", and its width W and height H. That is, the clip is

$$Q = \begin{pmatrix} P_{x_0-\frac{H}{2},y_0-\frac{W}{2}} & \cdot & \cdot & \cdot & P_{x_0-\frac{H}{2},y_0+\frac{W}{2}} \\ \cdot & \cdot\cdot & \cdot & \cdot\cdot & \cdot \\ \cdot & \cdot & P_{x_0,y_0} & \cdot & \cdot \\ \cdot & \cdot\cdot & \cdot & \cdot\cdot & \cdot \\ P_{x_0+\frac{H}{2},y_0-\frac{W}{2}} & \cdot & \cdot & \cdot & P_{x_0+\frac{H}{2},y_0+\frac{W}{2}} \end{pmatrix} \qquad (4)$$

The alignment mark is usually found by searching for a pixel that satisfies some given conditions. In this particular pattern, the alignment mark is defined as the pixel that is equidistant to the two resist lines. Here the distance of a point p to a set of points B is defined as $d(p;B) = \min\{|\ p-b\ | \,|\, \forall b \in B\}$. If more than one pixel satisfies the condition, their mass center is taken as the alignment mark. The alignment mark in Fig. 1(d) is marked by "*".

Note that the extraction process for a SEM picture is conducted only once, thus the computational complexity is not of particular concern.

After the above four steps, a black/white image Q has been obtained, which will be compared with simulated images. Note that by the above method of choosing pattern edges, the filled patterns will be bordered by the outmost edges. This means Q is corresponding to the profile at the bottom of the remaining resist.

III. SEM/SIM COMPARATOR AND MODEL TUNER

Given a simulation output, no matter if it is an aerial image or an activated site concentration, it can be treated with a threshold model to obtain a monochromatic representation of the resist patterns after development. This means resist for which the simulated value is higher than a given threshold is considered to dissolve, and otherwise the resist is considered to remain.

For the purpose of comparing SEM's with simulatio n, it is necessary to clip the simulated image with the same window defined in Section II, step 4. The clipping process is essentially identical. Note that in the presence of lens aberration, the simulated image is no longer symmetric, thus the coordinates of the alignment mark can not be determined in advance of simulation.

The clipped simulated image is denoted as R, which is also a black/white image. After obtaining the monochromatic representations of the SEM picture and simulated image, namely Q and R, the Image Mismatching Factor (IMF), a 2D metric evaluating the error of the simulation is defined as:

$$IMF = \frac{\sum_i \sum_j \left| R_{ij} - Q_{ij} \right|}{\sum_i \sum_j Q_{ij}} \qquad (5)$$

Note that the numerator represents the area in which the simulation does not agree with the SEM picture, whereas the denominator represents the area of the resist patterns in the SEM picture. An example of comparing a SEM with the simulation is shown in Fig. 2.

The simulation model can now be optimized using this metric. The optimization process is depicted in Fig. 3. The simulation is iterated with a different set of parameters until IMF is minimized.

IV. ANALYSIS OF SEVERAL SIMULATION MODELS

Using the above SEM/SIM comparison/tuning methodology, several levels of physical assumptions in simulation models were tested and evaluated. All the models were optimized with the pattern shown in Fig. 1. The separation between the line ends is 170nm, and the linewidth is 150nm. OPC has been applied to the mask. The true dimensions were measured and used in the simulation. The patterns were illuminated with a 193nm scanner, NA 0.6, σ 0.75, resist thickness 350nm and BARC thickness 82nm. The patterns were exposed at 5 defocus levels, -0.2, -0.2, 0, 0.1, 0.2 μm. Therefore the training set has 5 SEM pictures corresponding to the 5 defocuses.

1) Aerial Image Model without Lens Aberrations. Given the mask data, the 2D aerial image is obtained from image simulator which in this case was SPLAT. In this model, the only adjustable parameter is the intensity threshold. In Fig. 4 the simulations are overlaid with SEM clips. They agree in the white area while disagree in the gray area. The mean IMF of Aerial Image Model is 0.4.

2) Aerial Image Model with Lens Aberrations. In this model, the lens aberration data measured on the exposure tool were included in the image simulation. The overlay of SEM images and simulations is shown in Fig. 5. The mean IMF of 0.14 is significantly lower than without the aberration model.

3) Imaging in Resist Model. The second model was further refined by simulating the image intensity within the resist by using SPLAT. Since the SEM clips obtained in Section II are actually the very bottom of the resist profile, the image intensity distribution at just above the bottom plane of the resist layer is calculated to represent the resist patterns. The overlay of SEM images and simulations using this model is shown in Fig. 6. The mean IMF is 0.129, 8% smaller than the IMF of the second model.

4) Basic Post Exposure Bake Model. This model converts the image intensity from the third model into photoacid concentration using Dill's ABC model [5]. The photoacid concentration profile is then input into RIAR, a fast post exposure bake (PEB) simulator [6], to obtain the activated site concentration distribution, which is then used to predict the resist patterns after development. A threshold level of deprotection after the PEB simulation is used to predict the printed pattern shape. The initial post exposure bake model was measured at International SEMATECH. Fig. 7 shows the overlay of SEM and simulation. The mean IMF is 0.136, and is unexpectedly higher than the third model. The difference in IMF, however, is sufficiently small to be considered as noise due to the small size of the training set.

5) Tuned Post Exposure Bake Model. This model uses the same simulation process as the 4th model, but the resist parameters were tuned to minimize the IMF. This is in accordance with the fact that the resist model parameters often vary from fab to fab. The overlay is shown in Fig. 8. The mean IMF is 0.133.

Fig. 9 is a plot of the IMF showing the cumulative effect of each component on the model. Adding lens aberrations reduces IMF by 0.26, adding resist optical parameters (i.e., Image in Resist Model) reduces IMF by 0.01, whereas adding and tuning resist PEB parameters in fact increasing the IMF by less than 0.005. This small increment could be attributed to noise.

Comparing the above five models, apparently the lens aberrations contribute most to the simulation error. Since the last three models give similar IMF, one might conclude that the resist PEB model plays only a minor role in predicting critical dimensions. This is not true, however, as will be shown in Section V.

V. PREDICTABILITY OF THE MODELS

To test the effectiveness of the last three models, the optimum parameters obtained in Section V were applied to simulate a smaller end-to-end pattern, whose spacing between the two ends is 120nm. Due to the small exposure latitude of this small feature, only three SEM pictures were taken, corresponding to –0.1, 0 and 0.1μm defocus. The comparison of SEM and simulations of the three models at the defocus of 0μm is shown in Fig. 10. The IMF vs. defocus curve is plotted in Fig. 11. It can be seen that the Tuned PEB Model agrees with SEM best, its IMF is 10% less than that of Basic PEB Model. The IMF of the Basic PEB Model is now 20% smaller than the IMF of Image in Resist Model. Even though they has been similar in the "training stage". Thus it is concluded that adding resist PEB model will significantly improve the predictability of the simulation model. This is not surprising in that even though the optics contribute the most to the feature distortion, the acid diffusion/reaction process, whose effective path is less than tens of nanometers, will play an important role in feature distortion when the feature size is approaching 100nm.

VI. CONCLUSION

The algorithm for extracting monochromatic representation of resist patterns from SEM pictures worked well. At present the computational complexity of the algorithm is not critical since it needs to be run only once for each SEM picture. The Image Mismatching Factor (IMF), introduced as a 2-dimensional metric for evaluating the simulation model performance, also worked well and allowed a framework for tuning simulation models to be built.

On the basis of the above methodology, several levels of physical assumptions in simulation models were optimized for an end-to-end pattern whose spacing between line-ends is 170nm, over 0.4μm defocus range. Their IMFs showed that the lens aberrations contribute the most to the feature distortion. After incorporating lens aberration, the IMF drops from 0.4 to 0.14. The Image in Resist Model, which includes the resist optical character (refractive index, Dill's ABC parameters), further reduces the IMF to 0.129. Adding resist PEB model parameters were provided by SEMATECH causes an unexpected slight rise of IMF. Tuning resist PEB parameters did not improve IMF, either. However, the tuned resist model did significantly improve the predictability of the simulation when applied to small patterns whose spacing between line-ends is 120nm. Specifically, the IMF of Tuned PEB Model is 28% smaller than that of the Image in Resist Model, which indicates that a resist PEB model is indispensable for a predicative lithographic simulator.

ACKNOWLEDGEMENT

All the experiments were done in Texas Instruments. The authors deeply appreciate Keeho Kim and Maureen Hanratty for directing the project, Mark Terry for providing the lens aberrations, Jerry Schlesinger for helping with the SEM, and Mark Ma for helping on mask measurement. The authors also would like to thank Jeff Byers of International SEMATECH for providing basic resist parameters.

The lithography research was supported by industry and the State of California under the SMART program SM97-01.

REFERENCE

[1] T A. Brunner, Proc. of SPIE, Vol. 2726, pp 198-207, 1996

[2] C A. Mack, "*Line end shortening (lithography)*", Microlithography World, Vol. 9, (No. 2), Spring 2000

[3] J. Byers, Proc. SPIE, Vol. 2724, pp 156-162, 1996

[4] M. Zuniga et al, J. Vac. Sci. Tech. B, Dec 95 (2957)

[5] E. Croffie et al, SPIE Vol. 3678, 1999

[6] M. Cheng et al, SPIE Vol. 3999, pp. 854-864, 2000

[7] M. Cheng et al, SPIE Vol. 3678, pp.128, 1999

[8] Jae Lim, "*Two-Dimensional Signal and Image Processing*", Prentice Hall, 1990

[9] Donald Hearn and M. Baker, "*Computer Graphics*", 2nd Ed., Prentice Hall, 1994

[10] E. Croffie et al, Microelectronic Engineering, Vol. 53, June 2000, pp437-442

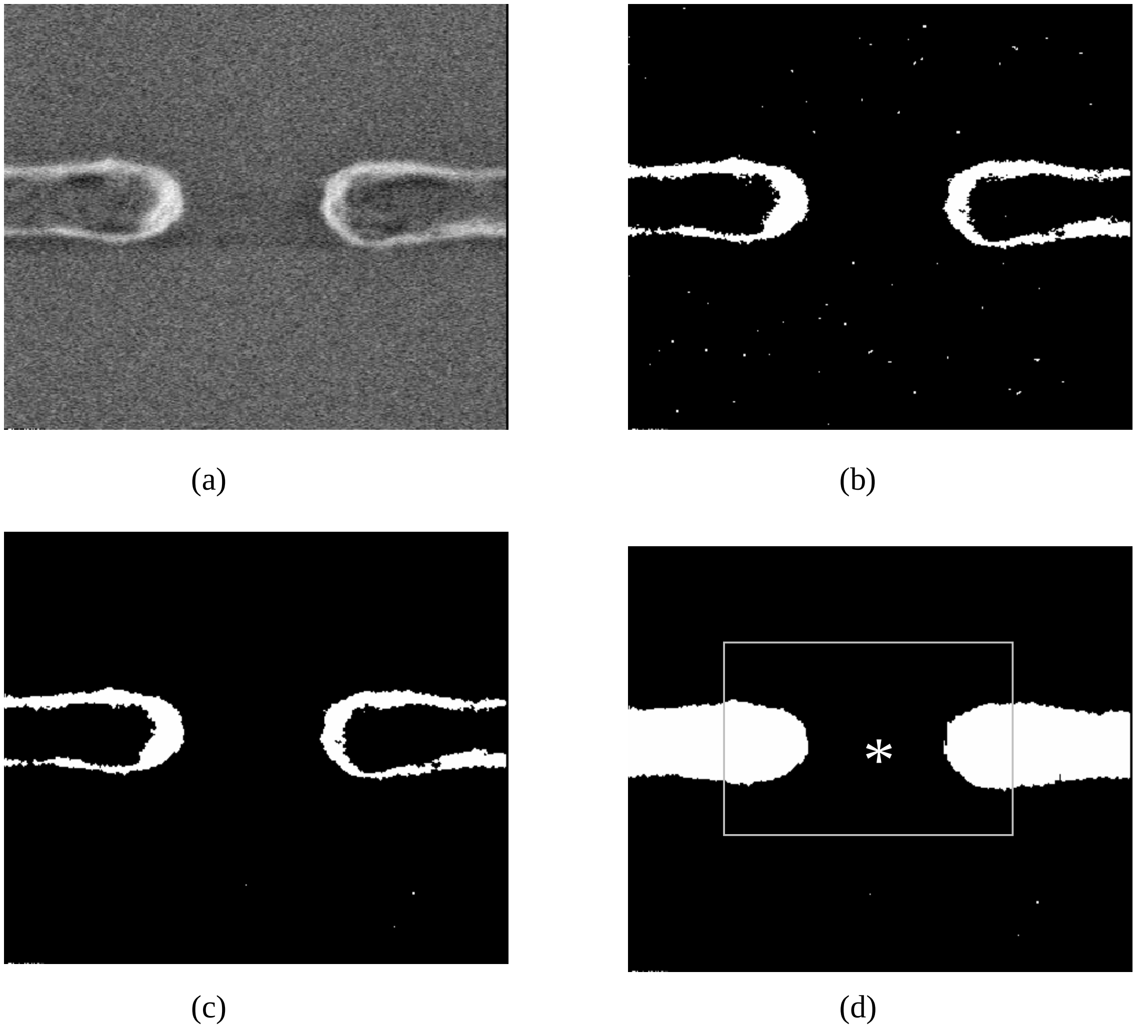

Fig. 1. The process of extracting black/white representations from SEM pictures. (a) SEM picture, (b) image after extracting the edges, (c) image after removal of noise, (d) image after filling the area inside the edges. In (d) the alignment mark is highlighted by "*".

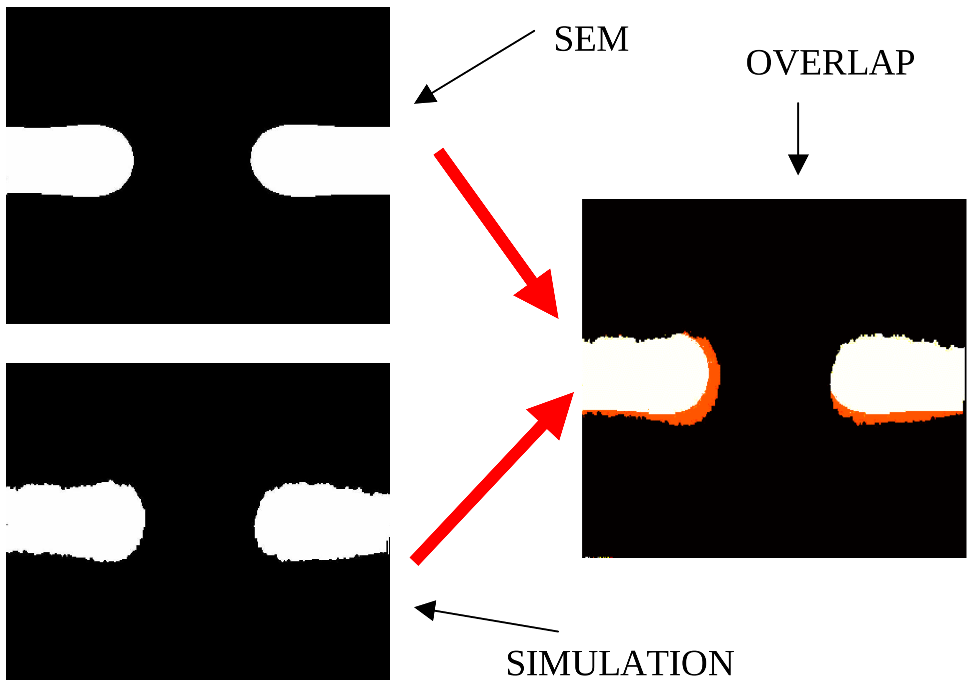

Fig. 2. Overlaying SEM with simulated image. The Image Mismatching Factor (IMF) is defined as the ration of the dark area in the overlap to the white area of the SEM.

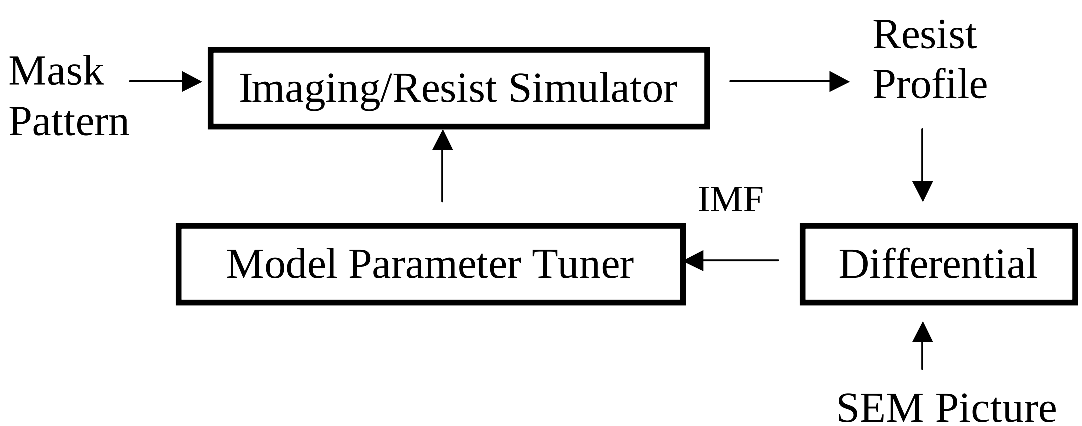

Fig. 3. The framework for tuning simulation models based on minimizing IMF.

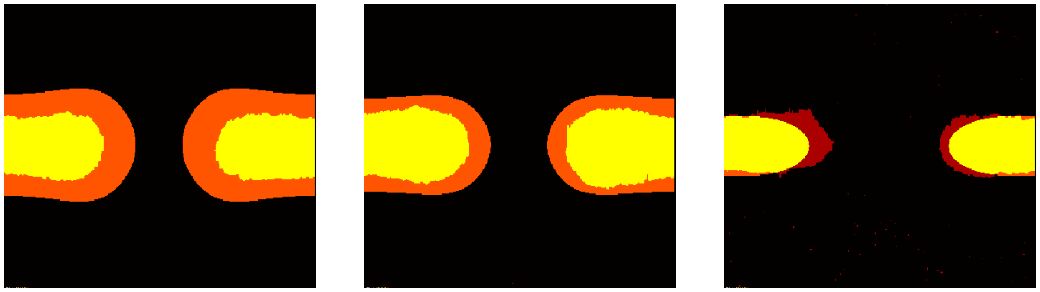

Fig. 4. Aerial Image Model without Lens Aberrations. From left to right, the defocuses are –0.2, 0, 0.2μm.

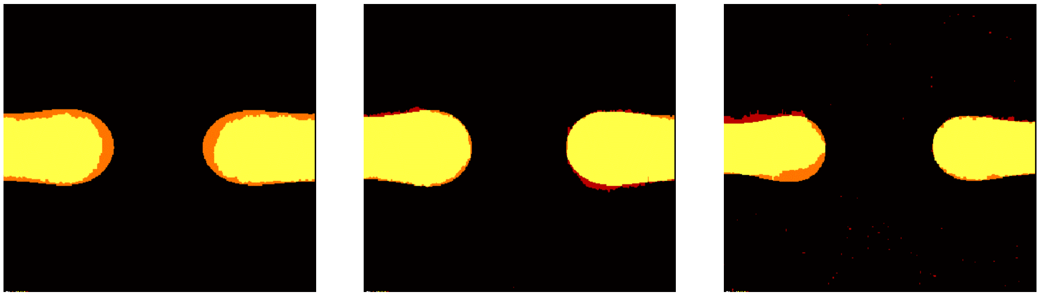

Fig. 5. Aerial Image Model with Lens Aberrations. From left to right, the defocuses are –0.2, 0, 0.2μm.

Fig. 6. Image in Resist Model. From left to right, the defocuses are –0.2, 0, 0.2μm.

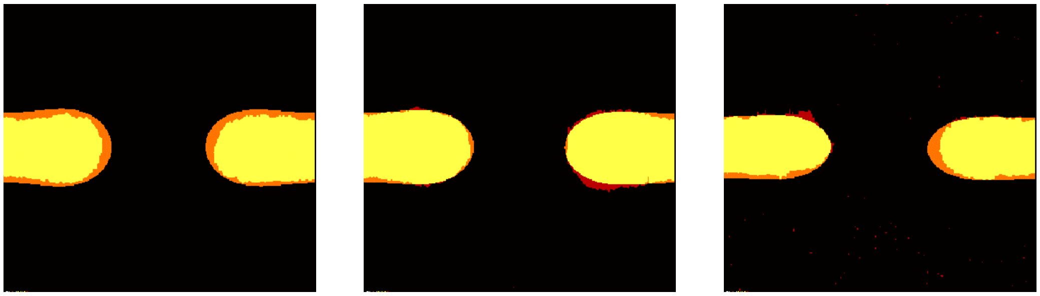

Fig. 7. Basic Post Exposure Bake Model. From left to right, the defocuses are –0.2, 0, 0.2μm.

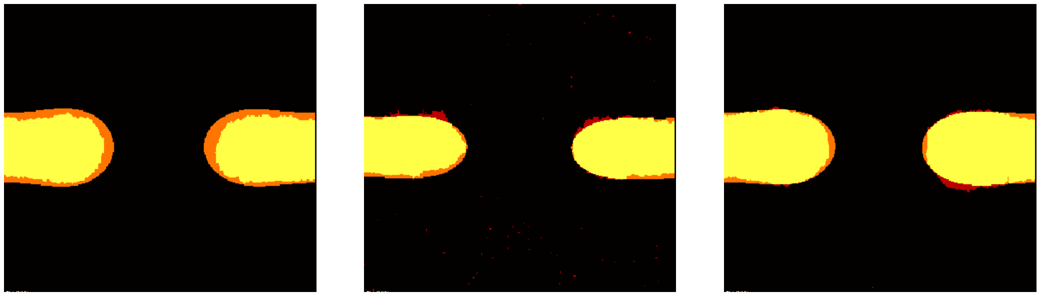

Fig. 8. Tuned Post Exposure Bake Model. From left to right, the defocuses are –0.2, 0, 0.2μm.

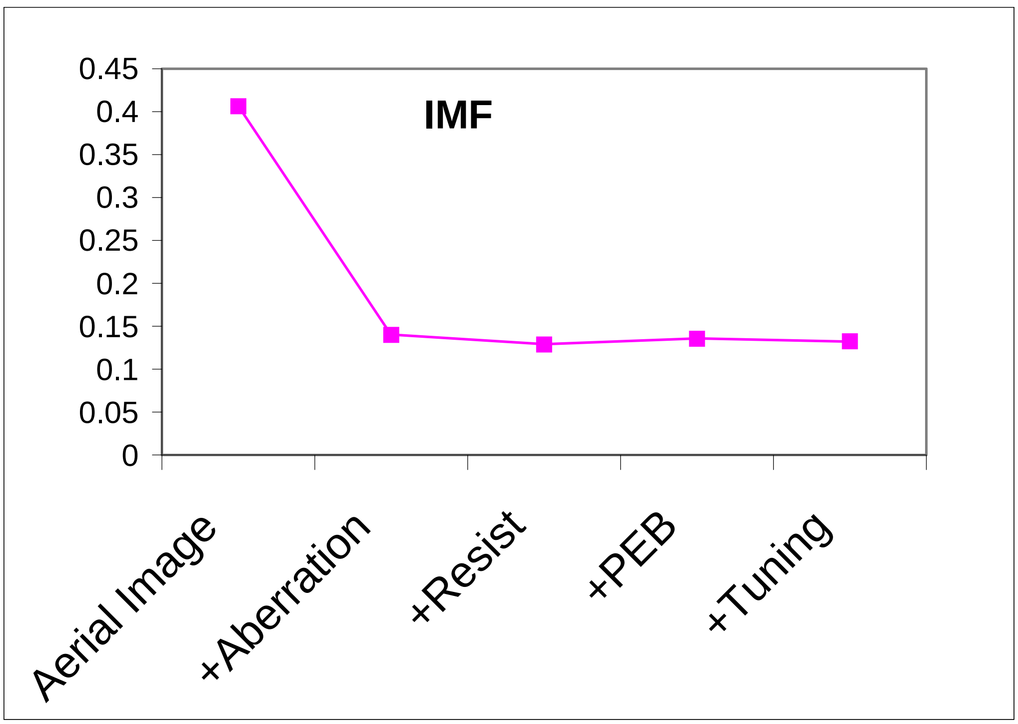

Fig. 9. Comparison of the performance of different models. It can be seen that lens aberration contributes most to the simulation performance.

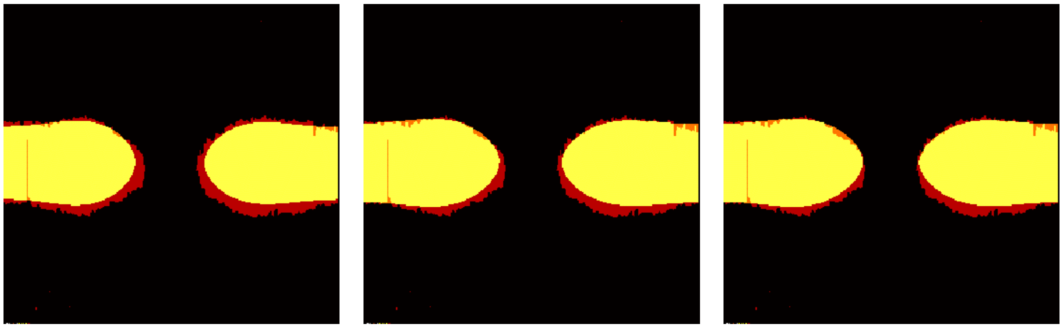

Fig. 10. Overlap of simulations with SEM. From left to right are the Image in Resist Model, Basic PEB Model and Tuned PEB Model, respectively, at the defocus of 0μm.

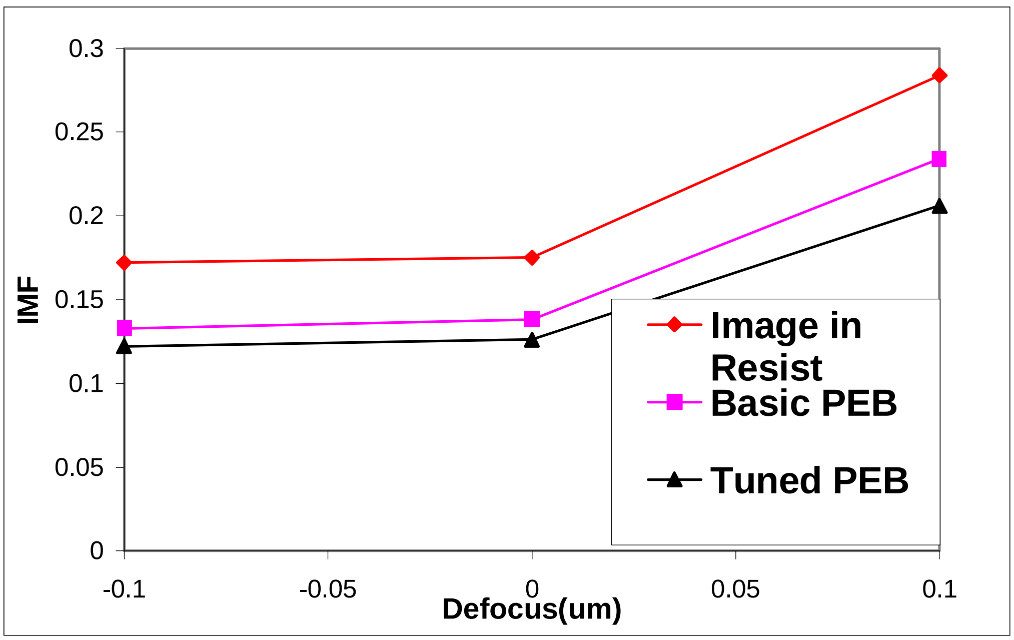

Fig. 11. Comparison of the predictive performance of different models. The Tuned PEB Model achieves the best predictability even though its IMF in training stage is not the best.